JACS
JOURNAL OF THE AMERICAN CHEMICAL SOCIETY
Communication
pubs.acs.org/JACS

Hydrogen Generation Catalyzed by Fluorinated Diglyoxime–Iron Complexes at Low Overpotentials

Michael J. Rose, Harry B. Gray, and Jay R. Winkler*

Beckman Institute, California Institute of Technology, Pasadena, California 91125, United States

Supporting Information

ABSTRACT: Fe^{II} complexes containing the fluorinated ligand 1,2-bis(perfluorophenyl)ethane-1,2-dionedioxime (dAr^FgH_2; H = dissociable proton) exhibit relatively positive $Fe^{II/I}$ reduction potentials. The air-stable difluoroborated species $[(dAr^FgBF_2)_2Fe(py)_2]$ (**2**) electrocatalyzes H_2 generation at −0.9 V vs SCE with $i_{cat}/i_p \approx 4$, corresponding to a turnover frequency (TOF) of ∼20 s^{-1} [Faradaic yield (FY) = 82 ± 13%]. The corresponding *mono*fluoroborated, proton-bridged complex $[(dAr^Fg_2H\text{-}BF_2)Fe(py)_2]$ (**3**) exhibits an improved TOF of ∼200 s^{-1} ($i_{cat}/i_p \approx 8$; FY = 68 ± 14%) at −0.8 V with an overpotential of 300 mV. Simulations of the electrocatalytic cyclic voltammograms of **2** suggest rate-limiting protonation of an $Fe^{"0"}$ intermediate ($k_{RLS} \approx 200$ M^{-1} s^{-1}) that undergoes hydride protonation to form H_2. Complex **3** likely reacts via protonation of an Fe^I intermediate that subsequently forms H_2 via a bimetallic mechanism ($k_{RLS} \approx$ 2000 M^{-1} s^{-1}). **3** catalyzes production at relatively positive potentials compared with other iron complexes.

The production of H_2 from proton sources is a major goal of contemporary energy science.[1] Pt is the most efficient catalyst, but its low abundance and high cost prohibit its widespread use. Researchers have investigated alternative alloys,[2] materials,[3] and molecules[4−7] to achieve H_2 generation using more abundant elements. In seminal work, DuBois and co-workers reported that Ni and Co phosphines exhibit high turnover frequencies (TOFs) of 10^3–10^5 s^{-1} at low overpotentials (50–400 mV).[6] Co diglyoximes[7] also operate at low overpotentials with high rates,[4,5] and considerable effort has been directed toward elucidating the mechanisms employed by these catalysts.[8] Peters and co-workers[4] and Fontecave and Artero[5] have established some of the factors that facilitate H_2 catalysis in tetraimine systems, such as a diglyoximato proton bridge.[5] More recently, polypyridine Co complexes reported by Chang[9] as well as our group[10] have been shown to catalyze H_2 evolution from aqueous systems. Although both Co and Ni are more abundant than Pt, a more attractive candidate for the catalytic metal center is Fe, the most abundant transition metal.

Early work by Saveánt on an Fe porphyrin, [(TPP)Fe(Cl)] (TPP = tetraphenylporphyrin), showed that H_2 could be produced at very negative $Fe^{II/I}$ potentials (below −1.5 V vs SCE)[11a] with reasonable catalytic rates (Table 1). More recently, Ott and co-workers reported that mononuclear $[(o\text{-ndt})Fe(PMe_3)_2(CO)_2]$ (*o*-ndt = *o*-napthalenedithiolate) also catalyzes H_2 evolution at similar potentials.[12] Biomimetic diiron

Table 1. Reported Fe Complexes for Electrocatalytic H_2 Production[a]

catalyst	peak E_{cat}	i_{cat}/i_p	ref
$[(dArFg_2H\text{-}BF_2)Fe(py)_2]$ (**3**)	−0.8	8	this work
$[(dArFgBF_2)_2Fe(py)_2]$ (**2**)	−0.9	4	this work
[(TPP)Fe(Cl)]	−1.6	∼10	11a
$[(o\text{-ndt})Fe(PMe_3)_2(CO)_2]$	−1.4	∼10	12a
μ-pdt$[Fe(CO)_3][Fe(CO)_2IMes]$	−1.9	∼4	13a
$[Fe_2(S_2C_3H_6)(CO)_3(dpv)NO]^+$	−0.8	∼2	14a
μ-$(SC_6H_4\text{-}2(CO)S)[Fe_2(CO)_6]$	−0.9	<2	19
$(\mu\text{-pdt})[Fe_2(CO_5)PPyr_3]$	−1.3	<2	20
$[(P^{Ph}{}_2N^{Ph}{}_2)Ni]^{2+}$	−0.4	∼20	6e
$[(dmgBF_2)_2Co(MeCN)_2]$	−0.65	∼40	4a
$[(P^{Ph}{}_2N^{Ph})Ni]^{2+}$	−0.8	38	6a

[a] Potentials are in V vs SCE; peak E_{cat} and i_{cat}/i_p are for a scan rate of 100 mV/s.

systems pioneered by Darensbourg,[13] Rauchfuss,[14] and others[15−17] electrocatalyze H_2 production at potentials in the range −1 to −2 V vs SCE. For example, $(\mu\text{-}S(CH_2)_3S)[Fe(CO)_3][Fe(CO)_2IMes]$ [IMes =1,3-bis(2,4,6-trimethylphenyl)-imidazol-2-ylidene] catalyzes H_2 generation near −2 V vs SCE;[13] the nitrosylated complex $[Fe_2(S_2C_3H_6)(CO)_3(dppv)(NO)]^+$ [dppv = *cis*-1,2-bis(diphenylphosphinoethylene)], which possesses an $Fe^{II/I}$ couple slightly positive of −1 V vs SCE, shows limited catalytic activity.[14] Lichtenberger and co-workers have summarized the functional [Fe–Fe] models,[18] including contributions from their laboratory. In separate work, Sun and Peng reported that complexes with more weakly donating dithiolates[19] in $(\mu\text{-}SC_6H_4\text{-}2\text{-}(CO)S\text{-}\mu)[Fe_2(CO)_6]$ or ancillary phosphines[20] in $(\mu\text{-pdt})[Fe_2(CO)_5PPyr_3]$ (pdt = propanedithiolate; PPyr = tripyrrolylphosphine) exhibit $Fe^{II/I}$ couples closer to −1 V vs SCE but have limited catalytic activity [peak catalytic current/noncatalytic current ratio (i_{cat}/i_p) < 2]. Overall, because of the inherent limitations of the $[\mu\text{-}S_2\text{–}Fe_2]$ scaffold and negative $Fe^{II/I}$ reduction potentials, there is no example of a biomimetic Fe catalyst that operates at reasonable potentials (E_{cat} > −1 V vs SCE) *and* exhibits high i_{cat}/i_p values.

Fe analogues of cobaloximes ($[(dRg)Fe(L)_2]$; dRg = disubstituted glyoxime; R = CH_3, C_6H_5; L = MeCN, pyridine, imidazole) have been reported by Stynes,[21] but very negative $[(L)Fe]/[(L)Fe]^-$ reduction potentials (−1.8 V vs SCE) render them unsuitable for H_2 catalysis. We reasoned that dramatic modifications of the dianionic ligand could mitigate

Received: January 17, 2012
Published: May 14, 2012

dx.doi.org/10.1021/ja300534r | J. Am. Chem. Soc. 2012, 134, 8310–8313

such negative reduction potentials. Here we report the syntheses of fluorinated Fe complexes with $[(L)Fe]/[(L)Fe]^-$ reduction potentials more positive than −1 V vs SCE that catalyze the production of H_2 from trifluoroacetic acid (TFA) in CH_2Cl_2 (or MeCN) solution.

Reaction of aqueous glyoxal with $NH_2OH{\cdot}HCl$ precipitates glyoxime, which can then react with $Cl_2(g)$ in aqueous HCl to afford dichloroglyoxime (dCl_2gH_2) in moderate yield (40% for two steps; Scheme 1). Treatment of dCl_2gH_2 with the Grignard reagent derived from pentafluorobromobenzene (Ar^FMgBr, generated with 1 equiv of ^{i}PrMgBr) affords dAr^FgH_2 in good yield (65%).

Scheme 1. Synthesis of dAr^FgH_2

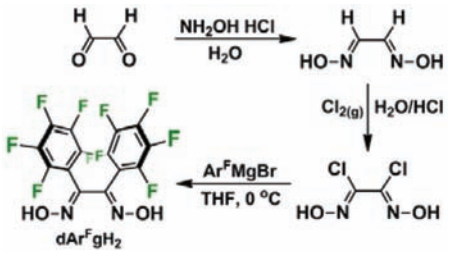

Metalation of dAr^FgH_2 (2 equiv) with Fe^{II} acetate in MeCN containing 5 equiv of pyridine (py) proceeded smoothly to afford gram quantities of an air-stable violet solid, $[(dAr^FgH)_2Fe(py)_2]$ (**1**), in good yield (73%); recrystallization from $CHCl_3$/pentane afforded X-ray-quality crystals (wR_2 = 0.0416, $P2_1/c$). In the structure of **1** (Figure 1, top), the Fe

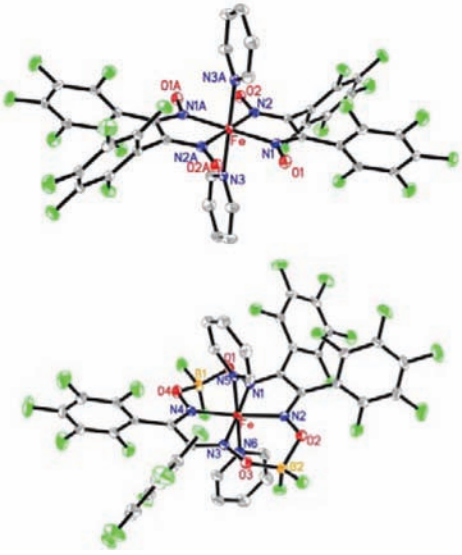

Figure 1. ORTEP diagrams of (top) **1** and (bottom) **2** (50% ellipsoids; H atoms omitted for clarity).

center is in a plane of symmetry, with $Fe-N_{gly}$ distances [1.896(1) and 1.901(1) Å] significantly shorter than those in the related nonfluorinated complex $[(dpgH)_2Fe(3\text{-}MePy)_2]$ (1.976 Å).[22] The pyridines [$Fe-N_{py}$ = 2.001(1) Å] are in a parallel orientation, similar to those in $[(dpgH)Fe(3\text{-}MePy)_2]$.[22] The IR spectrum of **1** exhibits ν_{CN} at 1524 cm^{-1}, which is red-shifted relative to free dAr^FgH_2 (ν_{CN} = 1658 cm^{-1}). Solutions of **1** in CD_3CN or CD_2Cl_2 exhibit sharp ^1H and ^{19}F NMR peaks in the diamagnetic region, consistent with a low-spin Fe^{II} ground state. Red-violet solutions of **1** in CH_2Cl_2 exhibit an intense feature at 560 nm [ε = 11 200 M^{-1} cm^{-1}; Figure S1 in the Supporting Information (SI)], which we assign to a metal-to-ligand charge transfer (MLCT). The cyclic voltammogram (CV) of **1** in CH_2Cl_2 exhibits a reversible $Fe^{III/II}$ couple at +0.83 V vs SCE and two irreversible reductions at −1.57 and −1.87 V vs SCE (Figure S2). Such negative potentials prompted further modification to bring the reduction potential into a reasonable range for H_2 electrocatalysis.

Reaction of **1** with 6 equiv of $BF_3{\cdot}Et_2O$ in 1:3 MeCN/Et_2O followed by workup in $CHCl_3$/py (10:1) afforded a bluish-violet solution. Vapor diffusion of pentane crystallized the difluoroborated complex $[(dAr^FgBF_2)_2Fe(py)_2]$ (**2**) as violet needles (wR_2 = 0.0425, $P\bar{1}$). The crystal structure of **2** (Figure 1, bottom) reveals fluoroboration of both glyoxime moieties, resulting in macrocyclic chelation of the Fe center. The $Fe-N_{gly}$ bond distances [1.881(1) and 1.884(1) Å] are slightly shorter than those in **1**, likely as a result of macrocyclic encapsulation; they are also shorter than those in the closely related complex $[(dmgBF_2)_2Fe(py)_2]$ [$Fe-N_{gly}$ = 1.905(5)].[23] The axial pyridines in **2** adopt a perpendicular orientation, as found in $[(dmgBF_2)Fe(py)_2]$, with distinct axial $Fe-N_{py}$ distances [1.998(1) vs 2.042(1) Å] due to steric effects associated with the tilting of the two BF_2 groups downward toward one py moiety.

In the solid state, ν_{CN} of **2** is blue-shifted to 1558 cm^{-1} due to the presence of the electron-withdrawing BF_2 groups (ν_{BF} = 1100 cm^{-1}). Violet solutions of **2** exhibit a red-shifted MLCT band at 570 nm (ε = 14 700 M^{-1} cm^{-1}, CH_2Cl_2; Figure S1) and sharp ^1H and ^{19}F NMR peaks in the diamagnetic region ($CDCl_3$ or CD_3CN). Solutions of **2** are air-stable, and electrochemical experiments revealed no $Fe^{III/II}$ couple up to +1.5 V vs SCE, indicating a highly stabilized Fe^{II} center. Complex **2** exhibits an irreversible reduction at −0.71 V, followed by a reversible redox couple at −0.94 V (Figure S3). The oxidation wave near +0.5 V was observed only after proceeding through the one-electron reduction, and all three features originate from solution processes, as determined by the scan rate (ν) dependence (linear i_p vs $\sqrt{\nu}$ plot; Figure S4). The CV of **2** could be simulated (DigiElch) by a model that included rapid loss of pyridine (K_{eq} = 1 × 10^7 M^{-1} and k_{off} = 500 s^{-1}) upon reduction of Fe^{II} to Fe^{I} (Scheme S1A in the SI).

To test the catalytic ability of **2**, we obtained CVs at different TFA concentrations. Figure 2 shows a systematic increase in i_{cat} observed near −0.9 V with increasing acid concentration from 0.1 to 50 mM (Figure S5; [**2**] = 0.5 mM). The resulting i_{cat}/i_p value of ∼4 is higher than that for any reported diiron model complex at equivalent potentials, such as $[Fe_2(S_2C_3H_6)(CO)_3(dppv)(NO)]^+$ or $(\mu\text{-}SC_6H_4\text{-}2\text{-}(CO)S\text{-}\mu)[Fe_2(CO)_6]$ (both i_{cat}/i_p < 2).[14,19] The i_{cat}/i_p versus [TFA] plots for **2** (low [TFA], linear region) as a function of ν (Figure S6) gave a TOF lower limit of ∼25 s^{-1}. The i_{cat}/i_p value exhibited by **2** is, however, lower than those of some molecular Ni/Co systems in organic solvents: $[(dmgBF_2)_2Co(MeCN)_2]$ ($i_{cat}/i_p \approx 30$); $[(PPh_2NPh)_2Ni]^{2+}$ (**38**); $[(P^{tBu}{}_2N^{Ph}{}_2)Co(MeCN)_3]^{2+}$ (**40**).[4,6]

CVs in MeCN (where E°_{TFA} = −0.51 V vs SCE and pK_a = 12.0; Figures S7 top, S12, and S14)[24] gave nearly identical E_{cat} and i_{cat}/i_p values, suggesting an overpotential of 400 mV for **2**. Bulk electrolysis of **2** (at −0.95 V vs SCE) with 30 mM TFA resulted in a relatively linear charge-pass plot (Figure 2 inset) over the course of the first hour (2.6 mol of H_2 mol^{-1} h^{-1}; 90% activity retained; 30% activity at 3 h), with an 82 ± 13% Faradaic yield (FY) of H_2 production. We also simulated the

dx.doi.org/10.1021/ja300534r | J. Am. Chem. Soc. 2012, 134, 8310−8313

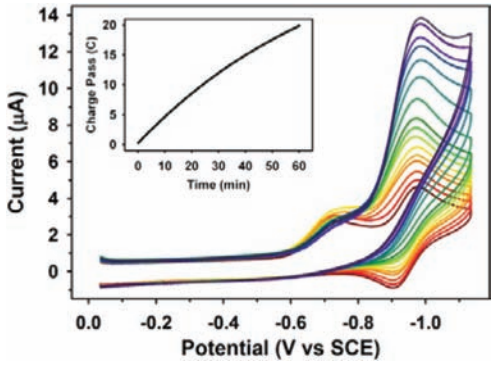

Figure 2. CVs for **2** in CH_2Cl_2 with increasing [TFA]. Experimental parameters: 0.5 mM **2**, 0−45 mM TFA; 100 mV/s, 0.1 M NBu_4ClO_4; glassy carbon (GC) working electrode (WE), Ag/AgCl reference electrode (RE), Pt counter electrode (CE). Inset: Charge pass for bulk electrolysis of **2** in MeCN (30 mM TFA).

catalytic CVs of **2** (DigiElch; Scheme S1B and Figure S8). As the catalytic intermediate is a two-electron-reduced complex (putative $Fe^{"0"}$), the data are consistent with a model involving slow protonation of $Fe^{"0"}$ to form Fe^{II}−H ($k_{RLS} \approx 200\ M^{-1}\ s^{-1}$) followed by rapid protonation of the hydride to form H_2 and Fe^{II}. A similar mechanism has been invoked in the Co−$dmgBF_2$ system at high acid concentrations.[8] Neither experimental nor simulated plots of k_{obs} versus [TFA] (Figure S13) displayed a simple first- or second-order dependence on [TFA], suggesting that k_{obs} is a composite of elementary rate constants. Simulations suggested that the acid-independent region (high [TFA]) is not rate-limited by dissociation of py upon reduction of **2**.

During the course of our synthetic work, we isolated an intermediate in the fluoroboration reaction that proved to be an asymmetric complex (Figure 3). This reaction, in which only

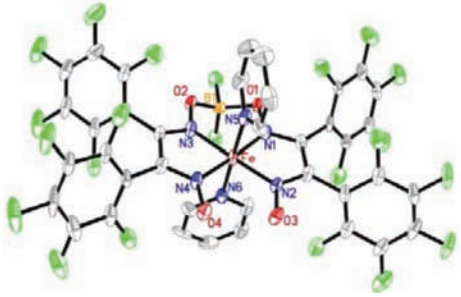

Figure 3. ORTEP diagram of **3** (50% ellipsoids; H atoms omitted for clarity).

one side of the diglyoxime complex underwent fluoroboration (4 equiv of $BF_3{\cdot}Et_2O$, 2 h, 1:3 MeCN/Et_2O), afforded violet crystals of [(dAr^Fg_2H-BF_2)Fe(py)$_2$] (**3**) (wR_2 = 0.067, $P2_1/c$), wherein the proton bridge between O3 and O4 is retained. The bond distances and angles about the Fe center and the spectroscopic properties of **3** (diamagnetic ^1H and ^{19}F NMR; λ_{max} = 565 nm, ε = 9780 $M^{-1}\ cm^{-1}$; ν_{CN} = 1529 cm^{-1}) are similar to those of **2**.

Asymmetric fluoroborated complexes are exceedingly rare,[25] but **3** is isolable because of the low reactivity due to the presence of the four Ar^F groups. Fontecave and Artero noted the importance of maintaining a proton bridge in [(DO)(DOH)^{Pr}Co(Br)$_2$], [DO = *N*,*N*-propanediylbis(2,3-butadione-2-imine-3-oxime)] versus the corresponding complex [$((DO)_2BF_2)^{Pr}Co(Br)_2$] that does not have −OH groups proximal to the metal center.[5] Additionally, DuBois and co-workers emphasized the value of a proton relay in their investigation of complexes containing PNP, P2N2, and P2N ligands.[6]

The CV of **3** (Figure 4, dark-red line) exhibits reduction waves at −0.93 and −1.14 V vs SCE (a pattern similar to **2**),

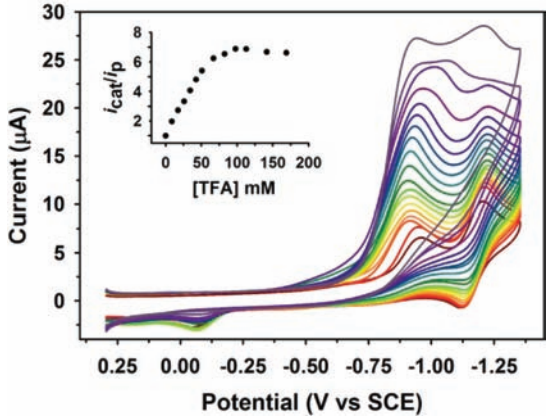

Figure 4. CVs of **3** in CH_2Cl_2 solution with increasing [TFA]. Inset: Dependence of i_{cat}/i_p on [TFA]. Experimental parameters: 0.5 mM **3**, 0−170 mM TFA; 100 mV/s, 0.1 M NBu_4ClO_4; GC WE, Ag/AgCl RE, Pt CE.

with the latter being reversible ($E_{1/2}$ = −1.08 V; Scheme S2A). CVs in the presence of increasing [TFA] indicate H_2 generation, with catalytic onset coinciding with the first reduction wave (−0.9 V). At higher [TFA] (>75 mM), catalysis was also observed at the second reduction wave, contributing an additional ∼10% to i_{cat}. The operating potential for **3** in the presence of TFA (−0.8 V) is shifted 100 mV positive versus the $Fe^{II/I}$ potential in the absence of acid, possibly because of substitution of py (protonated by TFA; see Scheme S2B). Catalyst **3** remains active at higher acid concentrations (>150 mM) than for **2** (50 mM) (Figure 4 inset and Figure S11). The i_{cat}/i_p value (∼8, FY = 68 ± 14%, 2.9 mol of H_2 mol^{-1} h^{-1} for the first hour) is twice that for **2** (i_{cat}/i_p = 4) and roughly an order of magnitude greater than those of other Fe catalysts that operate at similar potentials. Indeed, **3** retains a greater extent of activity than **2** after 1 h (99 vs 90%; Figure S9) and after 3 h (70 vs 30%). Indeed, the only comparable i_{cat}/i_p values are exhibited by [(TPP)Fe(Cl)] and [(*o*-ndt)Fe$(PMe_3)_2(CO)_2$],[11,12] both of which operate at potentials ∼500 mV more negative than **2** or **3**. The E_{cat} exhibited by **3** (−0.8 V) suggests that it catalyzes H_2 production using TFA at an overpotential of only 300 mV, which is 100 mV less than that of [$(dmgBF_2)_2Co(MeCN)_2$] (E_{cat} = −0.65 V) with TosH (E°_{TosH} = −0.25 V).[24]

Simulations of the electrocatalytic CVs for **3** indicate an Fe^I species to be the primary active intermediate (Scheme S2B), consistent with the previously proposed bimetallic mechanism[4] (for Co^I) that relies on rate-limiting oxidative protonation of Fe^I to form an Fe^{III}−H intermediate, which rapidly decays through a bimetallic pathway to form H_2 and the Fe^{II} starting material. Although we could not simulate the CVs assuming a monometallic mechanism, we cannot rule out this possibility.[11d] Our simulation (Figure S10) suggests $k_{RLS} \approx 2000\ M^{-1}\ s^{-1}$ and a corresponding TOF of 200 s^{-1}; these values represent

dx.doi.org/10.1021/ja300534r | *J. Am. Chem. Soc.* 2012, 134, 8310−8313

a 10-fold enhancement in catalysis versus **2** ($k_{RLS} \approx 200\ M^{-1}\ s^{-1}$, TOF = 20 s^{-1}). In this respect, catalysts **2** ($Fe^{"0"}$ active species) and **3** (Fe^{I} active species) represent a unique opportunity to explore differing mechanisms within the same ligand/metal system at similar driving forces.

The lower activity of $dAr^{F}g$-derived Fe catalysts versus existing Co/Ni complexes may be substantially offset by the greater abundance and lower cost of iron. We are now exploring other electronic and structural modifications to the {$dAr^{F}gX$} (X = H, BF_2, BR_2) ligand system in attempts to achieve lower overpotentials and higher catalytic efficiencies.

■ ASSOCIATED CONTENT

Ⓢ Supporting Information

CIF for **1**−**3**; additional spectra, experimental and simulated CVs, and resulting analyses; and supporting reaction schemes. This material is available free of charge via the Internet at http://pubs.acs.org.

■ AUTHOR INFORMATION

Corresponding Author

winklerj@caltech.edu

Notes

The authors declare no competing financial interest.

■ ACKNOWLEDGMENTS

This work was supported by the NSF CCI Solar Fuels Program (CHE-0802907). M.J.R. was supported by an NSF ACC-F Fellowship (CHE-1042009). The Bruker APEXII diffractometer was obtained via an NSF CRIF:MU Award (CHE-0639094). We thank Larry Henling and Michael Day for solving the crystal structures.

■ REFERENCES

(1) (a) Walter, M. G.; Warren, E. L.; McKone, J. R.; Boettcher, S. W.; Mi, Q.; Santori, E. A.; Lewis, N. S. *Chem. Rev.* **2010**, *110*, 6446. (b) Lewis, N. S.; Nocera, D. G. *Proc. Natl. Acad. Sci. U.S.A.* **2006**, *103*, 15729. (c) Gray, H. B. *Nat. Chem.* **2009**, *1*, 7.

(2) Trasatti, S. *Adv. Electrochem. Sci. Eng.* **1992**, *2*, 1.

(3) (a) Woodhouse, M.; Parkinson, B. A. *Chem. Soc. Rev.* **2009**, *38*, 197. (b) Jaramillo, T. F.; Jørgenson, K. P.; Bonde, J.; Nielson, J. H.; Horch, S.; Chorkendorff, I. *Science* **2007**, *317*, 100. (c) Merki, D.; Fierro, S.; Vrubel, H.; Hu, X. *Chem. Sci.* **2011**, *2*, 1262.

(4) (a) Hu, X.; Brunschwig, B. S.; Peters, J. C. *J. Am. Chem. Soc.* **2007**, *129*, 8988. (b) Dempsey, J. L.; Brunschwig, B. S.; Winkler, J. R.; Gray, H. B. *Acc. Chem. Res.* **2009**, *42*, 1995. (c) Hu, X.; Cossairt, B. M.; Brunschwig, B. S.; Lewis, N. S.; Peters, J. C. *Chem. Commun.* **2005**, 4723.

(5) (a) Baffert, C.; Artero, V.; Fontecave, M. *Inorg. Chem.* **2007**, *46*, 1817. (b) Razavet, M.; Artero, V.; Fontecave, M. *Inorg. Chem.* **2005**, *44*, 4786. (c) Fourmond, V.; Jacques, P.-A.; Fontecave, M.; Artero, V. *Inorg. Chem.* **2010**, *49*, 10338. (d) Jacques, P.-A.; Artero, V.; Pécaut, J.; Fontecave, M. *Proc. Natl. Acad. Sci. U.S.A.* **2009**, *106*, 20627.

(6) (a) Helm, M. L.; Stewart, M. P.; Bullock, R. M.; Rakowski-DuBois, M.; DuBois, D. L. *Science* **2011**, *333*, 863. (b) Kilgore, U. J.; Roberts, J. A. S.; Pool, D. H.; Appel, A. M.; Stewart, M. P.; Rakowski-DuBois, M.; Dougherty, W. G.; Kassel, W. S.; Bullock, R. M.; DuBois, D. L. *J. Am. Chem. Soc.* **2011**, *133*, 5861. (c) Wiedner, E. S.; Yang, J. Y.; Dougherty, W. G.; Kassel, W. S.; Bullock, R. M.; Rakowski-DuBois, M.; DuBois, D. L. *Organometallics* **2010**, *29*, 5390. (d) Rakowski-DuBois, M.; DuBois, D. L. *Acc. Chem. Res.* **2009**, *42*, 1974. (e) Wilson, A. D.; Newell, R. H.; McNevin, M. J.; Muckerman, J. T.; Rakowski-DuBois, M.; Dubois, D. L. *J. Am. Chem. Soc.* **2006**, *128*, 358.

(7) (a) Schrauzer, G. N.; Windgassen, R. J. *J. Am. Chem. Soc.* **1966**, *88*, 3738. (b) Connolly, P.; Espenson, J. H. *Inorg. Chem.* **1986**, *25*, 2684.

(8) (a) Dempsey, J. R.; Winkler, J. R.; Gray, H. B. *J. Am. Chem. Soc.* **2010**, *132*, 1060. (b) Dempsey, J. R.; Winkler, J. R.; Gray, H. B. *J. Am. Chem. Soc.* **2011**, *132*, 16774.

(9) (a) Sun, Y.; Bigi, J. P.; Piro, N. A.; Tang, M. L.; Long, J. R.; Chang, C. J. *J. Am. Chem. Soc.* **2011**, *133*, 9212. (b) Bigi, J. P.; Hanna, T. E.; Harman, W. H.; Chang, A.; Chang, C. J. *Chem. Commun.* **2010**, *46*, 958.

(10) Stubbert, B.; Peters, J. C.; Gray, H. B. *J. Am. Chem. Soc.* **2011**, *133*, 18070.

(11) (a) Bhugun, I.; Lexa, D.; Saveánt, J.-M. *J. Am. Chem. Soc.* **1996**, *118*, 3982. (b) Saveánt, J.-M. *Chem. Rev.* **2008**, *108*, 2348. (c) Costentin, C.; Robert, M.; Saveánt, J.-M. *Acc. Chem. Res.* **2010**, *43*, 1019. (d) Andrieux, C. P.; Blocman, C.; Dumascouchiat, J. M.; Mhalla, F.; Saveánt, J.-M. *J. Electroanal. Chem.* **1980**, *113*, 19.

(12) (a) Kaur-Ghumaan, S.; Schwartz, L.; Lomoth, R.; Stein, M.; Ott, S. *Angew. Chem., Int. Ed.* **2010**, *49*, 8033. (b) Schwartz, L.; Singh, P. S.; Eriksson, L.; Lomoth, R.; Ott, S. *C. R. Chim.* **2008**, *11*, 875.

(13) (a) Tye, J. W.; Lee, J.; Wang, H.-W.; Mejia-Rodriguez, R.; Reibenspies, J. H.; Hall, M. B.; Darensbourg, M. Y. *Inorg. Chem.* **2005**, *44*, 5550. (b) Georgakaki, I. P.; Thomson, L. M.; Lyon, E. J.; Hall, M. B.; Darensbourg, M. Y. *Coord. Chem. Rev.* **2003**, *238*−*239*, 255. (c) Darensbourg, M. Y.; Lyon, E. J.; Smee, J. J. *Coord. Chem. Rev.* **2000**, *206*, 533.

(14) (a) Olsen, M. T.; Justice, A. K.; Gloaguen, F.; Rauchfuss, T. B.; Wilson, S. R. *Inorg. Chem.* **2008**, *47*, 11816. (b) Royer, A. M.; Stagni-Salomone, M.; Rauchfuss, T. B.; Meyer-Klaucke, W. *J. Am. Chem. Soc.* **2010**, *132*, 16997.

(15) Tard, C.; Pickett, C. J. *Chem. Rev.* **2009**, *109*, 2245.

(16) Fontecilla, J. C.; Ragsdale, S. W. *Adv. Inorg. Chem.* **1999**, *47*, 283.

(17) Ezzaher, S.; Orain, P.-Y.; Capon, J.-F.; Gloaguen, F.; Pétillon, F. Y.; Roisnel, T.; Schollhammer, P.; Talarmin, J. *Chem. Commun.* **2008**, 2547.

(18) Felton, G. A. N.; Mebi, C. A.; Petro, B. J.; Vannucci, A. K.; Evans, D. H.; Glass, R. S.; Lichtenberger, D. L. *J. Organomet. Chem.* **2009**, *17*, 2681.

(19) Wang, Z.; Jiang, W.; Liu, J.; Jiang, W.; Wang, Y.; Åkerman, B.; Sun, L. *J. Organomet. Chem.* **2008**, *693*, 2828.

(20) Huo, F.; Hou, J.; Chen, G.; Guo, D.; Peng, X. *Eur. J. Inorg. Chem.* **2010**, 3942.

(21) (a) Thompson, D. W.; Stynes, D. V. *Inorg. Chem.* **1990**, *29*, 3815. (b) Pang, I. W.; Stynes, D. V. *Inorg. Chem.* **1977**, *16*, 590.

(22) Dvorkin, A. A.; Simonov, Y. A.; Malinovskii, T. I.; Bulgak, I. I.; Batir, D. G. *Proc. Natl. Acad. Sci. USSR* **1977**, *234*, 1372.

(23) Vernik, I.; Stynes, D. V. *Inorg. Chem.* **1996**, *35*, 6210.

(24) (a) Felton, G. A. N.; Glass, R. S.; Lichtenberger, D. L.; Evans, D. H. *Inorg. Chem.* **2006**, *45*, 9181. (b) Eckert, F.; Leito, I.; Kaljurand, I.; Kütt, A.; Klamt, A.; Diedenhofen, M. *J. Comput. Chem.* **2008**, *30*, 799.

(25) Chmielewski, P. J. P.; Warburton, R. P.; Morales, L.; Stephenson, N. A.; Busch, D. H. *J. Coord. Chem.* **1991**, *23*, 91.